

Mas receptor is translocated to the nucleus upon agonist stimulation in brainstem neurons from spontaneously hypertensive rats but not normotensive rats

Flavia M. Cerniello^{1†}, Mauro G. Silva^{1†}, Oscar A. Carretero², and Mariela M. Gironacci^{1*}

¹Universidad de Buenos Aires, Facultad de Farmacia y Bioquímica, IQUIFIB (UBA-CONICET), Dpto. Química Biológica, Junín 956, 1113, Buenos Aires, Argentina; and ²Hypertension and Vascular Research Division, Henry Ford Hospital, Detroit, MI, USA

Received 28 June 2019; revised 31 October 2019; editorial decision 2 December 2019; accepted 9 December 2019; online publish-ahead-of-print 11 December 2019

Time for primary review: 36 days

Aims

Activation of the angiotensin (Ang)-(1-7)/Mas receptor (R) axis protects from sympathetic overactivity. Endocytic trafficking is an essential process that regulates receptor (R) function and its ultimate cellular responses. We investigated whether the blunted responses to Ang-(1-7) in hypertensive rats are associated to an alteration in MasR trafficking.

Methods and results

Brainstem neurons from Wistar-Kyoto (WKY) or spontaneously hypertensive rats (SHRs) were investigated for (i) Ang-(1-7) levels and binding and MasR expression, (ii) Ang-(1-7) responses (arachidonic acid and nitric oxide release and Akt and ERK1/2 phosphorylation), and (iii) MasR trafficking. Ang-(1-7) was determined by radioimmunoassay. MasR expression and functionality were evaluated by western blot and binding assays. MasR trafficking was evaluated by immunofluorescence. Ang-(1-7) treatment induced an increase in nitric oxide and arachidonic acid release and ERK1/2 and Akt phosphorylation in WKY neurons but did not have an effect in SHR neurons. Although SHR neurons showed greater MasR expression, Ang-(1-7)-elicited responses were substantially diminished presumably due to decreased Ang-(1-7) endogenous levels concomitant with impaired binding to its receptor. Through immunocolocalization studies, we evidenced that upon Ang-(1-7) stimulation MasRs were internalized through clathrin-coated pits and caveolae into early endosomes and slowly recycled back to the plasma membrane. However, the fraction of internalized MasRs into early endosomes was larger and the fraction of MasRs recycled back to the plasma membrane was smaller in SHR than in WKY neurons. Surprisingly, in SHR neurons but not in WKY neurons, Ang-(1-7) induced MasR translocation to the nucleus. Nuclear MasR expression and Ang-(1-7) levels were significantly greater in the nuclei of Ang-(1-7)-stimulated SHR neurons, indicating that the MasR is translocated with its ligand bound to it.

Conclusion

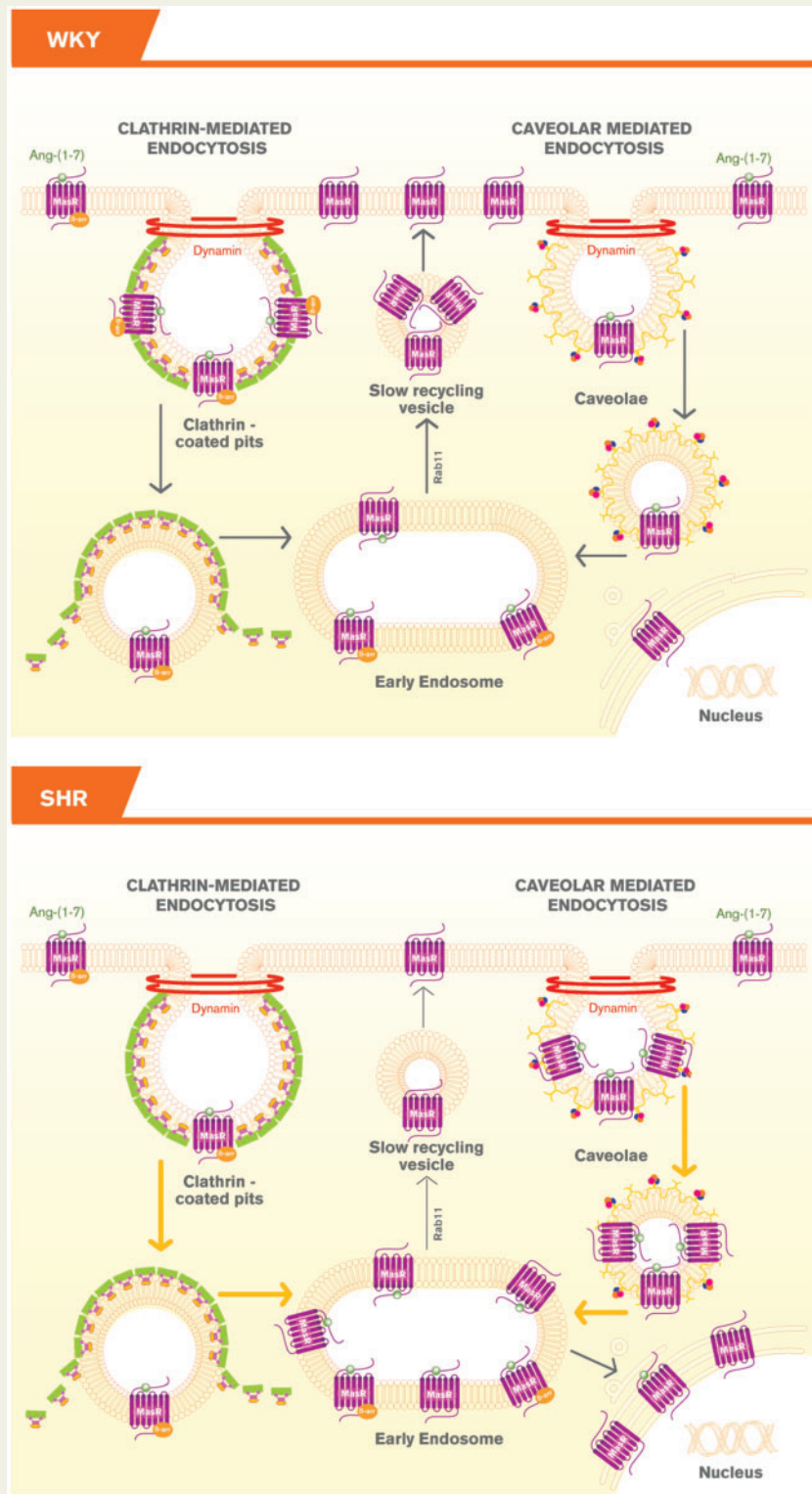
MasRs display differential trafficking in brainstem neurons from SHRs, which may contribute to the impaired responses to Ang-(1-7).

* Corresponding author. Tel: +54 11 496 48290; fax: +54 11 496 25457; E-mail: mariela@qb.fyb.uba.ar; marielagironacci@gmail.com

† The first two authors contributed equally to the study.

Published on behalf of the European Society of Cardiology. All rights reserved. © The Author(s) 2019. For permissions, please email: journals.permissions@oup.com.

Graphical Abstract



Keywords

Mas receptor • Hypertension • Receptor trafficking • Angiotensin-(1-7) • Neuron

1. Introduction

The brain renin–angiotensin system (RAS) plays an important role in sympathetic nervous system activity and arterial blood pressure regulation and hydrosaline homeostasis. Central RAS hyperactivity and sympathetic nervous system overactivity have been associated with hypertension among other diseases.¹ Centrally, angiotensin (Ang)-(1–7)/Mas receptor (R) represents the protective arm of the RAS and some of its protective actions may be attributed to its sympathoinhibitory actions.^{2,3} The spontaneously hypertensive rats (SHRs) are a well-established model for essential hypertension and brain disorders.^{4,5} Our previous evidence indicates that activation of Ang-(1–7)/MasR axis decreases sympathetic neurotransmission overactivity in SHRs.^{2,3}

Ang-(1–7) is the endogenous ligand for MasR, a G protein-coupled receptor (GPCR) expressed in the brain, among other tissues.^{2,3} After agonist binding, R activation and subsequent desensitization, several GPCRs are known to undergo endocytosis via clathrin-dependent or independent pathways.^{6,7} GPCRs are routed to the early endosome, where they are differentially sorted between recycling and degradative/lysosomal pathways, leading to signal re-sensitization or termination, respectively.^{6,7} The potential to re-programme GPCR signalling by modulating R trafficking or intracellular location is a key adaptive mechanism to maintain appropriate cellular function and homeostasis.⁶ Thus, R trafficking is not a universal mechanism for every R, and it critically determines the ultimate cellular response. In human embryonic kidney (HEK) cells 293T, MasR activation leads to β -arrestin2 recruitment followed by endocytosis through clathrin-coated pits (CCP) and caveolae into early endosomes and are then recycled back to the plasma membrane through slow recycling vesicles.^{8,9} Considering that abnormal GPCR trafficking leads to certain neurogenic disorders,^{6,10,11} we hypothesize that altered MasRs trafficking in sympathoexcitatory neurons in the brainstem may contribute to the elevated sympathetic outflow and to blunted responses to Ang-(1–7) in SHRs. The aim of this work was to investigate MasR endocytic trafficking in brainstem neurons from SHRs.

2. Methods

2.1 Reagents

Goat anti-mouse antibody coupled to Alexa 594 and Alexa 488, Dulbecco's modified Eagle's medium (DMEM) F12, B27, and LysoTracker Red were purchased from Invitrogen. Mouse anti-Rab11 (cat. 610656 lot. 45316), anti-EEA1 (cat. 610457 lot. 40486), anti-caveolin-1 (cat. 610406 lot. 2440), anti-AP50 (cat. 611350 lot. 30350), and anti-Nup62 (610497 lot. 3200765) antibodies were purchased from BD Biosciences. Ang-(1–7) was from Bachem. Rabbit anti-MasR was from Novus (cat. NLS1-1531 lot. 5831/32AP3-2 for immunofluorescence whose specificity was previously validated¹² and cat. NBP1-78444 lot. A-2 for western blot (antibody specificity presented in see [Supplementary material online, Figure S1](#)). (Rhod)-Ang-(1–7) was from Phoenix Peptides. Monoclonal mouse anti- β -arrestin2 (sc-13140 lot. K1914) was from Santa Cruz Biotechnology. Rabbit anti-ERK1/2-phosphoThr202/Tyr204 (cat. 9101S lot. 26), rabbit anti-Akt-phospho Ser473 (9271S lot. 12), rabbit anti-ERK1/2 (cat. 9102S lot. 23), and rabbit anti-Akt (cat. 9272S lot. 27) were from cell signalling. All other chemicals were analytical grade reagents of the highest purity available.

2.2 Animals

Newborn (1–3 days old) SHRs and their normotensive control Wistar-Kyoto (WKY) (Charles River Laboratories, Wilmington, MA, USA) or Sprague-Dawley (SD) rats were used in our study. The investigation conforms to the *Guide for the Care and Use of Laboratory Animals* published by the US National Institutes of Health (NIH Publication No. 85-23, revised 1996). The animal research protocol was approved by the Institutional Animal Care and Use Committee of the Faculty of Pharmacy and Biochemistry, University of Buenos Aires, Argentina (33074/2014).

To evaluate whether the hypertensive phenotype has impacted MasR and not simply strain difference, and because of a number of issues with WKYs,^{13,14} a set of experiments was performed with SD rats. It has been shown no difference between SD and WKY rats with regard to K^+ -stimulated norepinephrine release from the paraventricular hypothalamic nucleus,¹⁵ suggesting that neurons from both strains behave in the same manner.

2.3 Cell culture

Neurons from the brainstem were obtained from newborn rats as previously described,¹⁶ with slight modifications. Newborn rats were sacrificed by decapitation and the brainstem was dissected and dissociated in papain 18 U/mL (Worthington) at 37°C for 30 min. After being centrifuged 5 min at 600 \times g, the resultant pellet was triturated in DMEM containing DNase I (0.01 mg/mL) and centrifuged at 800 \times g for 5 min. Cells were resuspended in DMEM-F12 supplemented with B-27, GlutaMAX™-I (Gibco) and antibiotics and plated on poly-D-lysine pre-coated dishes. After 24 h, cytosine arabinoside (10 μ mol/L) was added to avoid the growth of non-neuronal cells. After 48 h, the medium was replaced by fresh medium, and neurons were allowed to complete differentiation. Neurons were used after 14 days in culture. We and others have previously shown that neurons are mature under this condition.^{17–19} The treatment of cells was carried out in a 24-h serum-starved condition. Every experiment was carried out with neuronal cultures of both strains for each period of incubation in parallel. Two to three newborn rats render eight million cells. Data presented corresponds to independent neuronal cultures submitted to 15 or 30 min stimulation with 1 μ mol/L Ang-(1–7) and not to a pooled data.

2.4 Ligand concentration

Since we previously showed that 1 μ mol/L Ang-(1–7) induced MasR internalization in HEK293T cells,^{8,9} 1 μ mol/L of Ang-(1–7) was employed in all the experiments. In addition, through electrospray ionization-ion trap mass spectrometry we previously showed that Ang-(1–7) is degraded in hypothalamic and brainstem neurons from rats.¹⁶ Thus, high concentrations of this peptide were employed just to assure that they reach the receptor in amount enough to measure a response.

2.5 Ang-(1–7) and Ang II levels

Ang-(1–7) and Ang II levels were measured in cells and nuclear lysates as previously described.^{20,21} The number of cells employed was around 8 and 12 million to measure cellular and nuclear Angs levels, respectively. Cells or nuclei were homogenized in acid ethanol (0.1 mol/L HCl/80% ethanol) containing the renin inhibitor acetyl-His-Pro-Phe-Val-Statine-Leu-Phe (3 mmol/L), 0.44 mmol/L o-phenanthroline, 1 mmol/L Na^+ para-chloromercuribenzoate, 0.12 mmol/L pepstatin A, 25 mmol/L EDTA, and a cocktail of protease inhibitors (Calbiochem cat. 539134). Homogenates were centrifuged at 20 000 \times g for 30 min at 4°C.

Proteins in the supernatant were quantified. The supernatant was subsequently lyophilized and Angs extraction and recovery was performed as previously described.²⁰ The recovery was around 90–95%. Each sample was corrected for each recovery. Angs levels were quantified by radioimmunoassay using Angs labelled in our laboratory as previously described.²² Radioimmunoassay for Ang-(1-7) has been previously validated.¹⁶ Results were expressed as pg/mg protein.

2.6 Ang-(1-7) binding

Ang-(1-7) binding using rhodamine (Rhod)-Ang-(1-7) was performed as previously described.²³ Briefly, cells were incubated in assay buffer (phosphate-buffered saline 0.02 mol/L, pH 7.4, and containing 5% BSA and a protease inhibitor cocktail) for 15 min at 4°C. Cells for non-specific binding were incubated for 15 min at 4°C in the same assay buffer in the presence of 10 µmol/L Ang-(1-7). Subsequently, the cells were incubated with Rhod-Ang-(1-7) (6 nmol/L) in assay buffer for 1 h at 4°C. Cells were then rinsed (three times for 1 min in assay buffer), fixed with 4% paraformaldehyde and mounted on coverslips. Images were obtained with an Olympus Fluoview FV1000 spectral laser scanning confocal microscope with a 60× oil-immersion lens, using a 559 nm excitation. Fluorescence emission was collected between 650 and 750 nm and the intensity was quantified using ImageJ software (NIH). The imaging parameters were the same across the WKY and SHR groups.

2.7 Nitric oxide measurement

Nitric oxide (NO) was measured using the fluorescent probe 4-amino-5-methylamino-2', 7'-difluorofluorescein (DAF-FM) (Invitrogen) according to the manufacturer's instructions. Cells were incubated in the dark with 5 µmol/L DAF-FM in DMEM-F12 for 45 min at 37°C, washed with PBS and incubated for 30 min with fresh media. Cells were then incubated in the absence (control) or presence of 1 µmol/L Ang-(1-7) for 15 or 30 min. After the incubation time, the medium was discarded, and the cells were washed with PBS and fixed with 4% paraformaldehyde. Images were obtained by laser scanning confocal microscopy (Olympus Fluoview FV1000) equipped with an oil-immersion objective lens (60×) and fluorescence intensity was quantified using ImageJ software. The imaging parameters were the same across the WKY and SHR groups.

2.8 Arachidonic acid release

Arachidonic acid (AA) release was measured as previously described.^{9,23} Cells were labelled with [³H]AA (0.2 µCi/well) (Perkin Elmer) for 16 h. Cells were then washed with DMEM containing 2% BSA and incubated in the absence or presence of Ang-(1-7) (1 µmol/L) for 15 or 30 min at 37°C. Radioactivity in the supernatant was measured. For total cellular radioactivity, cells in each well were solubilized with 1 mol/L NaOH and counted. [³H]AA released into the medium was expressed as percent of the total cellular radioactivity and referred to as fractional release.

2.9 Western blot

A western blot was performed as previously described.^{9,24} After treatments, cells were homogenized in ice-cold buffer (pH 7.4) containing 24 mmol/L 4-(2-hydroxyethyl)-1-piperazineethanesulfonic acid (HEPES), 1 mmol/L EDTA, 2 mmol/L tetrasodium pyrophosphate, 70 mmol/L sodium fluoride, 1 mmol/L β-glycerophosphate, 1% Triton X-100, 1 mmol/L phenylmethanesulfonyl fluoride (PMSF), 10 µg/mL aprotinin, and a cocktail of protease inhibitors (Calbiochem cat. 539134). Equal amount of proteins were subjected to 10% SDS-PAGE and transferred electrophoretically to polyvinylidene difluoride membrane. Non-specific binding

sites on the membrane were blocked by incubation with 5% milk in Tris-buffered saline solution containing 0.1% Tween 20. Membranes were subsequently probed with anti-MasR antibody (dilution 1:500; antibody specificity is shown in see [Supplementary material online, Figure S1](#)). Protein loading was evaluated by stripping and reblotting membranes with anti-GAPDH antibody (dilution 1:1000) for cellular lysates or with anti-nucleoporin 62 (Nup62) antibody, a nuclear marker (dilution 1:500) for nuclear fraction lysates. To evaluate ERK1/2 and Akt activation, membranes were subsequently probed with rabbit anti-ERK1/2-phosphoThr202/Tyr204 (pERK1/2) (1/1000) or rabbit anti-Akt-phospho Ser473 (1/1000) to measure ERK or Akt phosphorylation, respectively, followed by incubation with goat anti-rabbit IgGs coupled to horseradish peroxidase. Total protein content (non-phosphorylated) was evaluated by stripping and reblotting membranes with anti-ERK1/2 (1/1000) or anti-Akt (1/1000) antibodies. Immunoreactive bands were visualized by chemiluminescence detection and quantified by densitometry. MasR expression was normalized to GAPDH in cell lysates and to Nup62 in nuclear fractions. Phosphorylated ERK1/2 or Akt was normalized to total ERK1/2 and Akt, respectively, and to GAPDH.

2.10 Immunocytochemistry

MasR trafficking was evaluated by immunocytochemistry as previously described.^{9,24} Cells were incubated in the absence or presence of 1 µmol/L Ang-(1-7) for different lengths of time (stated in Section 3). After two washes with PBS, cells were fixed with 4% paraformaldehyde, permeabilized with 0.2% Triton X-100 in PBS and incubated in blocking solution (PBS/0.2% Triton X-100/3% BSA) for 30 min at room temperature. Cells were then incubated with different primary antibodies: anti-MasR rabbit antibody (dilution 1:250) plus anti-EEA1 or anti-βarrestin2 or anti-caveolin-1 or anti-Rab11 or anti-Nup62 mouse monoclonal antibodies (dilution 1:150) overnight at 4°C. The samples were rinsed twice in PBS/0.2% Triton X-100 and exposed to the secondary antibody (anti-mouse IgG AlexaFluor 594 and anti-rabbit IgG AlexaFluor 488, dilution 1:200) for 2 h at room temperature. Nuclei were stained with Hoechst 33258. Non-specific immunostaining was determined in samples incubated in the absence of the primary antibody or with the primary antibody pre-absorbed with 10 µmol/L Ang-(1-7). To evaluate MasR targeting to lysosomes, colocalization between MasR and the lysosome marker LysoTracker Red (Thermo Fisher Scientific USA) was evaluated. Cells were incubated in the probe-containing growth medium for 45 min. The medium was replaced by fresh medium, and cells were incubated in the absence or the presence of 1 µmol/L Ang-(1-7) for 30 min. After two washes with PBS, cells were fixed with 4% paraformaldehyde and incubated with rabbit anti-MasR antibody (dilution 1:250). Anti-rabbit IgG AlexaFluor 488 (dilution 1:200) was used as the secondary antibody. Samples were mounted and then imaged using an Olympus Fluoview FV1000 spectral laser scanning confocal microscope with a 60× oil-immersion lens using dual excitation (473 and 559 nm). Due to the spectral properties of the scan head, fluorescence emission was collected between 520 and 550 nm for Alexa 488 and 600–660 nm for Alexa 594. Images were obtained using sequential scanning for each channel to eliminate cross-talk of the chromophores. The imaging parameters were the same across the WKY and SHR groups, that is, all the images were taken with the same laser potency, gain, and HV parameters. The MasR fraction in different cell compartments was quantified using the CellProfiler software (<http://www.cellprofiler.org/>). Overlay methods help to generate visual estimates of colocalization events in two-dimensional images; however, they neither reflect the three-dimensional nature of the biological probe nor the restrained resolution along the z-axis.²⁵ For that reason, the best way is to quantify

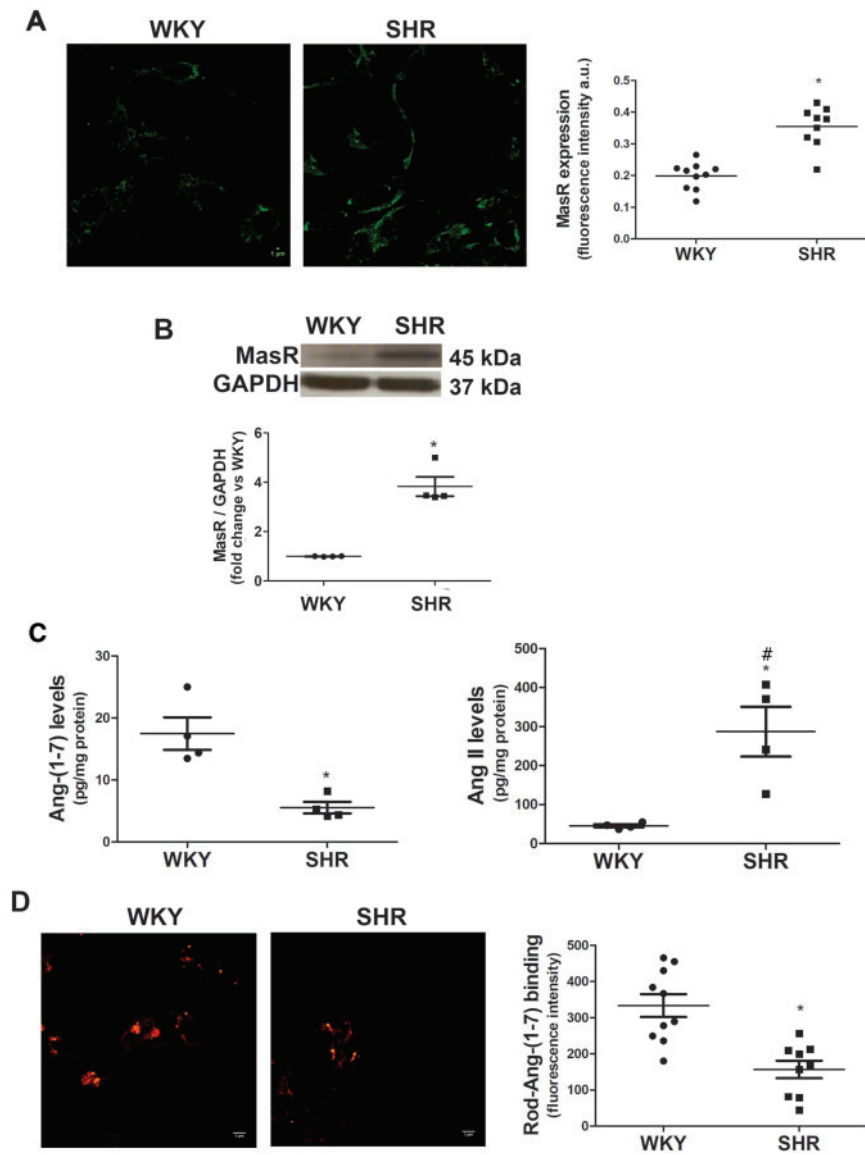


Figure 1 MasR expression is increased while Ang-(1-7) endogenous levels and binding are decreased in SHR brainstem neurons. (A) MasR expression measured by immunofluorescence. Representative images of MasR immunostaining (scale bar = 5 μ m) and quantification of MasR immunofluorescence in brainstem neurons from WKY and SHR (four to five images were analysed per independent neuronal culture; $n = 4$ independent neuronal cultures). Results were expressed as fluorescence intensity per cell (a.u.). (B) MasR expression measured by western blot ($n = 4$ independent neuronal cultures). A representative blot is presented. (C) Endogenous Ang-(1-7) and Ang II levels measured by radioimmunoassay ($n = 4$ independent neuronal cultures). Results are expressed as pg/mg protein. Data on Ang-(1-7) and Ang II levels were presented in separate graphs to make the difference in Ang-(1-7) levels in both strains be easily seen, although the statistical analysis was performed with all the data. (D) Representative images of Rhod-Ang-(1-7) binding and quantification of Ang-(1-7) binding expressed as fluorescence intensity per cell (a.u.) (four images were obtained per culture, $n = 3$ independent neuronal cultures). The line in each scatter plot shows the mean \pm SEM from independent neuronal cultures. WKY and SHR neuronal cultures were obtained in parallel. Each experiment was carried out with 500 000 cells (A and D) and eight million cells (B and C). Scale bar = 5 μ m. * $P < 0.05$ compared with the WKY group (Mann–Whitney non-parametric test or Kruskal–Wallis non-parametric tests followed by Dunn’s multiple comparison test in C); # $P < 0.05$ compared with Ang-(1-7) levels in WKY (one-way analysis of variance).

colocalization.^{25–27} All the images were obtained with the same microscope settings and all of them were used and analysed at the same time by the CellProfiler programme, thus there was not a bias in the results. The programme gives data about how much a signal colocalizes with another one. Results were expressed as the fraction of MasR that colocalizes with a particular marker, which is the ratio between the signals from MasR and the marker.

2.11 Nuclear fractionation

Nuclear fractions were obtained as previously described.²⁸ Cells were homogenized in hypotonic media (pH 7.4, 10 mmol/L HEPES, 10 mmol/L NaCl, 1 mmol/L KH_2PO_4 , 5 mmol/L NaHCO_3 , 5 mmol/L EDTA, 1 mmol/L CaCl_2 , 0, 5 mmol/L MgCl_2 , and protease inhibitor cocktail). After isotonic condition restoration with isotonic buffer (10 mmol/L HEPES, 10 mmol/L NaCl, 1 mmol/L KH_2PO_4 , 5 mmol/L NaHCO_3 , 5

mmol/L EDTA, 1 mmol/L CaCl₂, 0, 5 mmol/L MgCl₂, 250 mmol/L sucrose, and protease inhibitor cocktail), the samples were centrifuged at 6300 ×g for 5 min at 4°C, and the pellet was stored as the nuclear fraction. Nuclei were then lysed in a nuclear lysis buffer (pH 7.4, 24 mmol/L HEPES, 1 mmol/L EDTA, 1% Triton X-100 and protease inhibitor cocktail) and centrifuged at 13 000 ×g for 5 min at 4°C. The supernatant was collected, and proteins were quantified. Characterization of nuclear fraction was performed by measuring the expression of Nup62 (nuclear marker) and GAPDH (cytosolic marker) by western blot (see [Supplementary material online, Figure S2](#)).

2.12 Statistical analysis

Mann–Whitney non-parametric tests were used when comparing WKY rats and SHR. Kruskal–Wallis non-parametric tests followed by Dunn's multiple comparison tests were used when comparing different Ang-(1-7) treatments in a single strain. Prism 6 GraphPad software was used to perform statistical analyses. The results were considered significant at *P*-value of <0.05.

3. Results

3.1 MasR expression is increased and Ang-(1-7) endogenous levels are decreased in brainstem neurons from SHRs

MasR and Ang-(1-7) content in brainstem neurons derived from SHRs and their normotensive control WKY rats were determined. SHRs exhibited greater MasR expression compared with WKY (*Figure 1A* and *B*). Endogenous Ang-(1-7) levels were decreased while Ang II levels were increased in brainstem neurons from SHRs compared with those from WKY animals (*Figure 1C*) (Ang-(1-7) levels: 17.5 ± 2.6 pg/mg protein in WKY neurons and 5.9 ± 1.1 pg/mg protein in SHR neurons; Ang II levels: 45.7 ± 3.9 pg/mg protein in WKY neurons and 287.1 ± 64.0 pg/mg protein in SHR neurons). In addition, Ang II levels in SHRs neurons were significantly greater compared with those of Ang-(1-7). Regarding Ang-(1-7) binding, brainstem neurons from SHRs showed decreased Ang-(1-7) binding (*Figure 1D*).

3.2 Ang-(1-7) responses are decreased or absent in brainstem neurons from SHRs

AA release, NO generation, and Akt and ERK 1/2 phosphorylation were evaluated in neurons incubated in the absence or presence of Ang-(1-7) for 15 or 30 min. As shown in *Figure 2A*, basal AA release was higher in SHR neurons compared with WKY neurons. Ang-(1-7) induced a significant increase in AA release in WKY neurons, while a decrease in AA release in Ang-(1-7)-treated SHR neurons was observed.

Brainstem neurons from SHR exhibited lower basal NO levels compared with WKY neurons. Ang-(1-7) induced an increase in NO production only in WKY neurons but did not have an effect in neurons from SHRs (*Figure 2B*).

Basal Akt phosphorylation was greater in SHR than WKY neurons, while no difference in ERK1/2 phosphorylation between strains was observed (*Figure 2C* and *D*, respectively). Ang-(1-7) increased both Akt and ERK1/2 phosphorylation after 15 min stimulation in WKY neurons, but did not induce any significant change in neurons from SHRs (*Figure 2C* and *D*, respectively).

3.3 The internalized MasR fraction is greater in neurons from SHRs

β-arrestins promote GPCR internalization via coated pits by recruiting clathrin and clathrin adaptor protein-2.^{6,7} MasR immunostaining colocalized with β-arrestin2 in brainstem neurons from both WKY rats and SHRs after 15 min of stimulation with Ang-(1-7) (*Figure 3A*), suggesting a clathrin-mediated internalization. Quantification of colocalization showed that the fraction of MasRs that colocalized with β-arrestin2 was greater in neurons from SHRs compared with WKY rats under basal conditions (*Figure 3B*) suggesting that the amount of MasR being constitutively internalized through CCP was larger in SHR than in WKY neurons. Ang-(1-7) induced an increase in the fraction of MasRs that colocalized with β-arrestin2 in both strains and this effect was greater in WKY neurons compared with SHR (2.9- ± 0.2-fold increase in WKY neurons and 1.4- ± 0.3-fold increase in SHR neurons, *P* < 0.05; *Figure 3B* and see [Supplementary material online, Figure S3A](#)).

We evaluated whether MasRs were also internalized by caveolae. MasRs colocalized with caveolin-1, a specific marker for caveolae, in brainstem neurons from both strains after 15 min of stimulation with Ang-(1-7) (*Figure 3C*). Quantification of colocalization showed that the fraction of MasRs that colocalized with caveolin-1 was higher in the neurons from WKY animals than in those from SHRs under basal conditions (*Figure 3D*) suggesting a higher constitutive caveolae-mediated MasR internalization in WKY neurons. Ang-(1-7) induced an increase in MasR colocalization with caveolin-1 and this effect was greater in neurons from SHRs than from WKY animals (1.6- ± 0.2-fold increase in WKY neurons and 2.3- ± 0.3-fold increase in SHR neurons, *P* < 0.05) (*Figure 3D* and see [Supplementary material online, Figure S3B](#)).

To investigate whether MasRs were internalized into early endosomes, neuronal cells were stimulated with Ang-(1-7) for 15 min, and then colocalization of MasRs with the early endosome marker EEA1 was investigated. MasRs colocalization with the early endosomes marker EEA1 after 15 min Ang-(1-7) treatment was observed (*Figure 3E*). The fraction of MasRs present in the early endosomes was greater in neurons from SHRs than in neurons from WKY animals under basal conditions (*Figure 3F*). Ang-(1-7) induced an increase in the MasR fraction targeted to early endosomes and this increase was the same in both strains (2.4- ± 0.4-fold increase in WKY neurons and 2.3- ± 0.3-fold increase in SHR neurons) (*Figure 3F* and see [Supplementary material online, Figure S4](#)) but in the end the amount of MasR internalized was significantly greater in SHRs neurons.

Once internalized into early endosomes, the Rs may be targeted to lysosomes for complete degradation or be recycled back to the plasma membrane.^{6,7} Neuronal cells were incubated with Ang-(1-7) for 30 min, and colocalization of MasRs with the lysosome marker LysoTracker was investigated. MasRs did not colocalize with the lysosome marker in either WKY animals or SHRs (*Figure 4A*), demonstrating that the R is not directed to lysosomes for degradation. To investigate whether MasRs were recycled back to the plasma membrane, MasR colocalization with the slow recycling vesicle marker Rab11 was evaluated. As it is shown in *Figure 4B*, colocalization between MasR and Rab11 signals were observed. The fraction of MasRs that colocalized with Rab11 was similar in neurons from WKY rats and SHRs under basal conditions (*Figure 4C*). Ang-(1-7) induced an increase in the fraction of MasRs that colocalized with Rab11 in brainstem neurons from WKY rats and SHRs after 30 min treatment, but

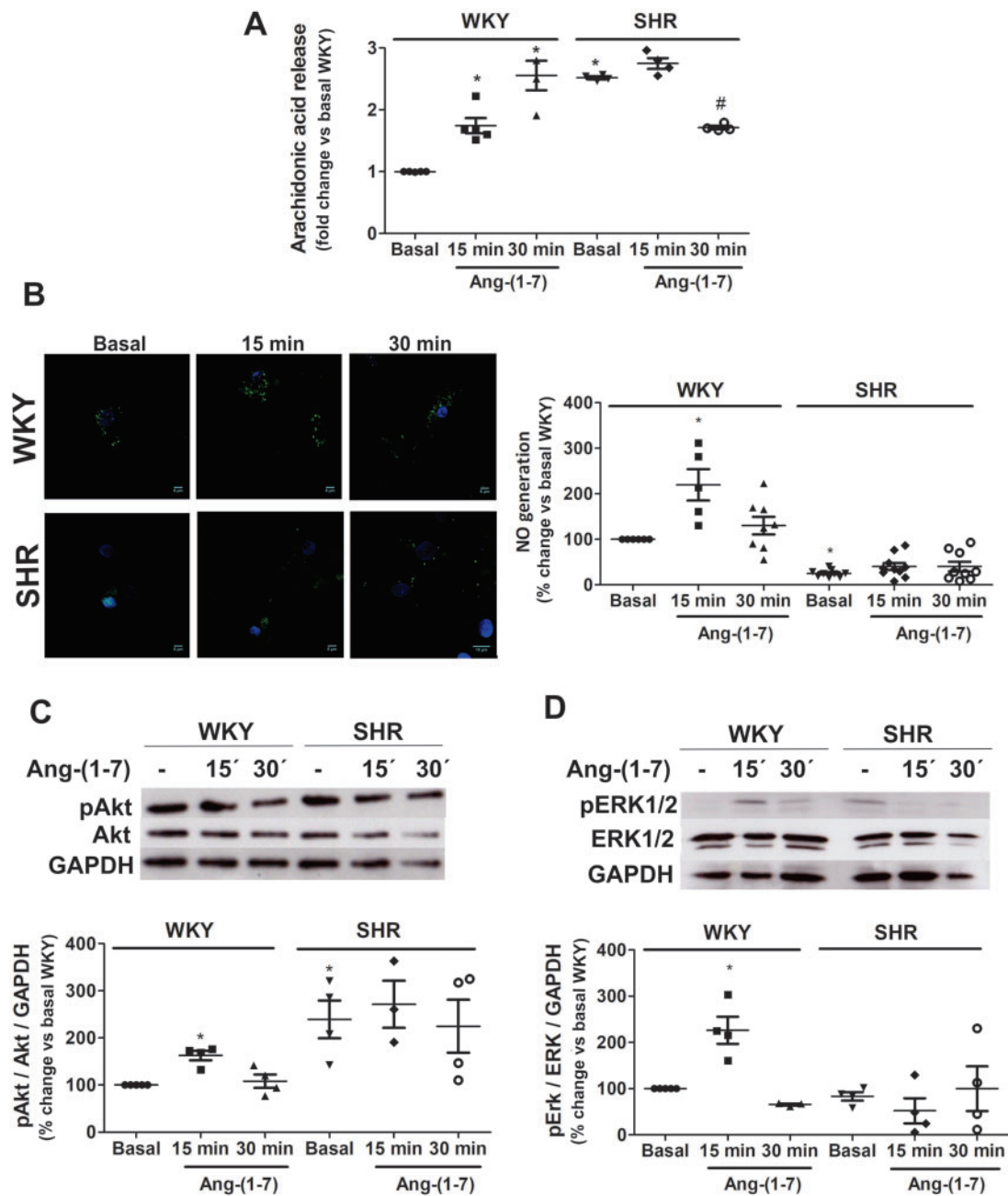


Figure 2 Ang-(1-7) responses are blunted in SHR neurons. AA release (A), NO generation (B), Akt phosphorylation (C), and ERK1/2 phosphorylation (D) were measured in brainstem neurons from WKY rats and SHRs incubated in the absence (basal) or presence of Ang-(1-7). Representative images of NO (NO in green and nucleus in blue) generation and representative western blots of total and phosphorylated Akt and ERK1/2 are presented in panels (B–D), respectively. The results are presented as changes in response relative to WKY neurons in the basal condition. The line in each scatter plot represents the mean \pm SEM of four independent neuronal cultures. Each experiment was carried out with 3.5 million (A), 500 000 (B) and eight million cells (C and D). * $P < 0.05$ vs. basal WKY; # $P < 0.05$ vs. basal SHR (Kruskal–Wallis non-parametric tests followed by Dunn’s multiple comparison tests).

this increase was smaller in neurons from SHRs (Figure 4C) suggesting that the fraction of MasR recycled back to the plasma membrane upon agonist stimulation was lower in SHR neurons.

Altogether, these results demonstrated that in brainstem neurons from WKY rats and SHRs, MasRs are internalized into early

endosomes upon agonist stimulation through CCP and caveolae and then are slowly recycled back to the plasma membrane. However, in the end, the fraction of internalized MasRs was greater and the number of Rs recycled back to the plasma membrane was smaller in neurons from SHRs.

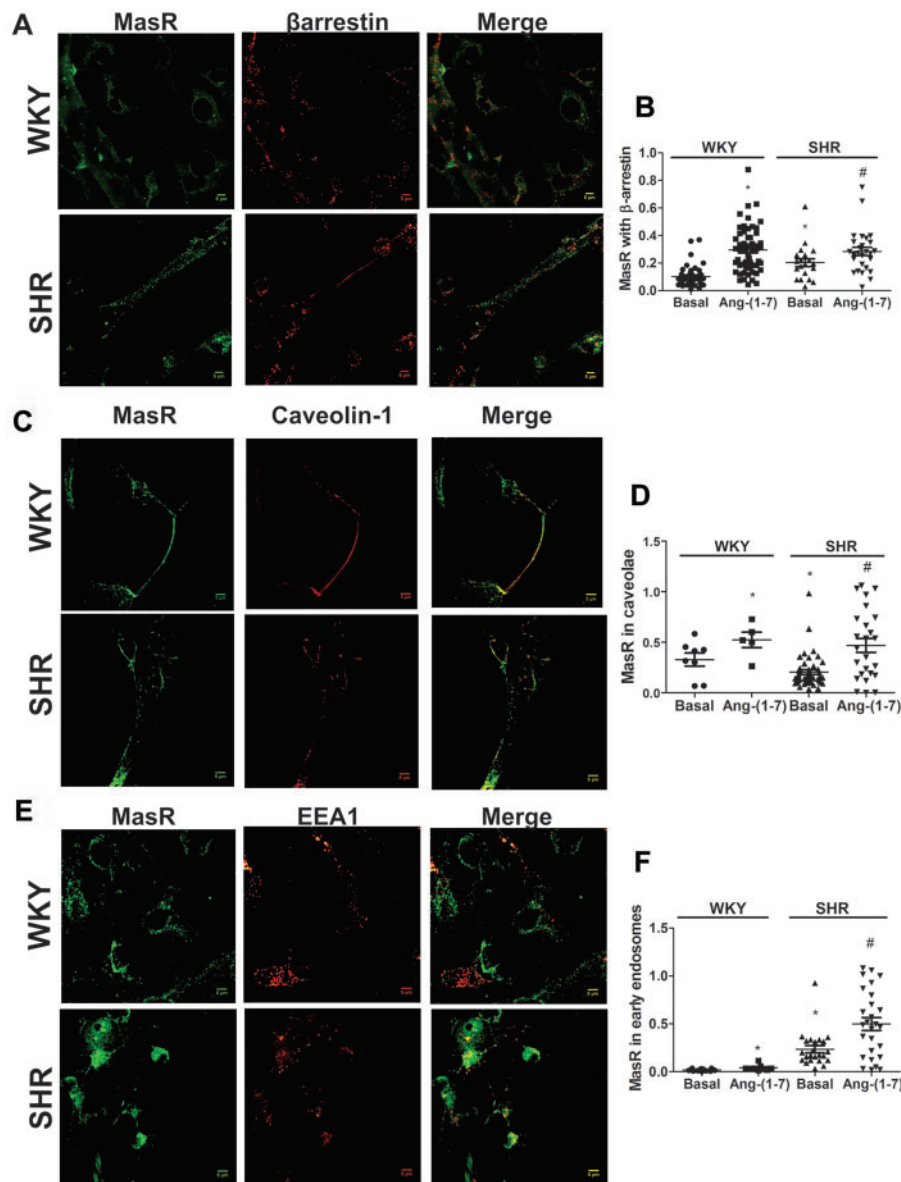


Figure 3 The internalized MasR fraction is greater in neurons from SHRs compared with WKY. Representative images of immunostaining of MasR (green) and β -arrestin2 (A), caveolin-1 (C), or the early endosome marker EEA1 (E; red) in brainstem neurons from WKY rats and SHRs stimulated with Ang-(1-7) for 15 min. Scale bar = 5 μ m. Quantification of MasR colocalization with β -arrestin2 (B), the caveola marker caveolin-1 (D), and the early endosome marker EEA1 (F) in brainstem neurons from WKY rats and SHRs incubated in the absence (basal) or the presence of Ang-(1-7) for 15 min. The line in each scatter plot represents the mean \pm SEM of the ratio between the signal from MasR and each marker. Four independent experiments were analysed (four to five images per experiment). Experiments were carried out with 500 000 cells for each condition. * $P < 0.05$ vs. basal WKY; # $P < 0.05$ vs. basal SHR (Kruskal–Wallis non-parametric tests followed by Dunn’s multiple comparison tests).

3.4 MasRs are translocated to the nucleus after agonist stimulation in neurons from SHRs

Several studies have demonstrated that GPCRs may localize and signal at the nucleus or may even be translocated to this intracellular compartment after agonist stimulation.^{29,30} MasR colocalization with a nuclear marker in WKY and SHR brainstem neurons, incubated in the absence or presence of Ang-(1-7) for 15 or 30 min, was analysed. MasRs colocalized with the nuclear marker under basal conditions (Figure 4E),

demonstrating that the R was constitutively expressed in the nucleus. The incubation of neuronal cultures with Ang-(1-7) for 30 min caused an increase in MasR colocalization with the nuclear marker in the nuclei of neurons from SHRs but not in those from WKY animals (Figure 4D), suggesting that the peptide induced MasR translocation to the nucleus. Lack of nuclear MasR translocation and the same MasR trafficking as in WKY neurons upon agonist stimulation was observed in brainstem neurons from SD rats (Figure 5) suggesting that the hypertensive phenotype has impacted MasR trafficking and not simply strain difference.

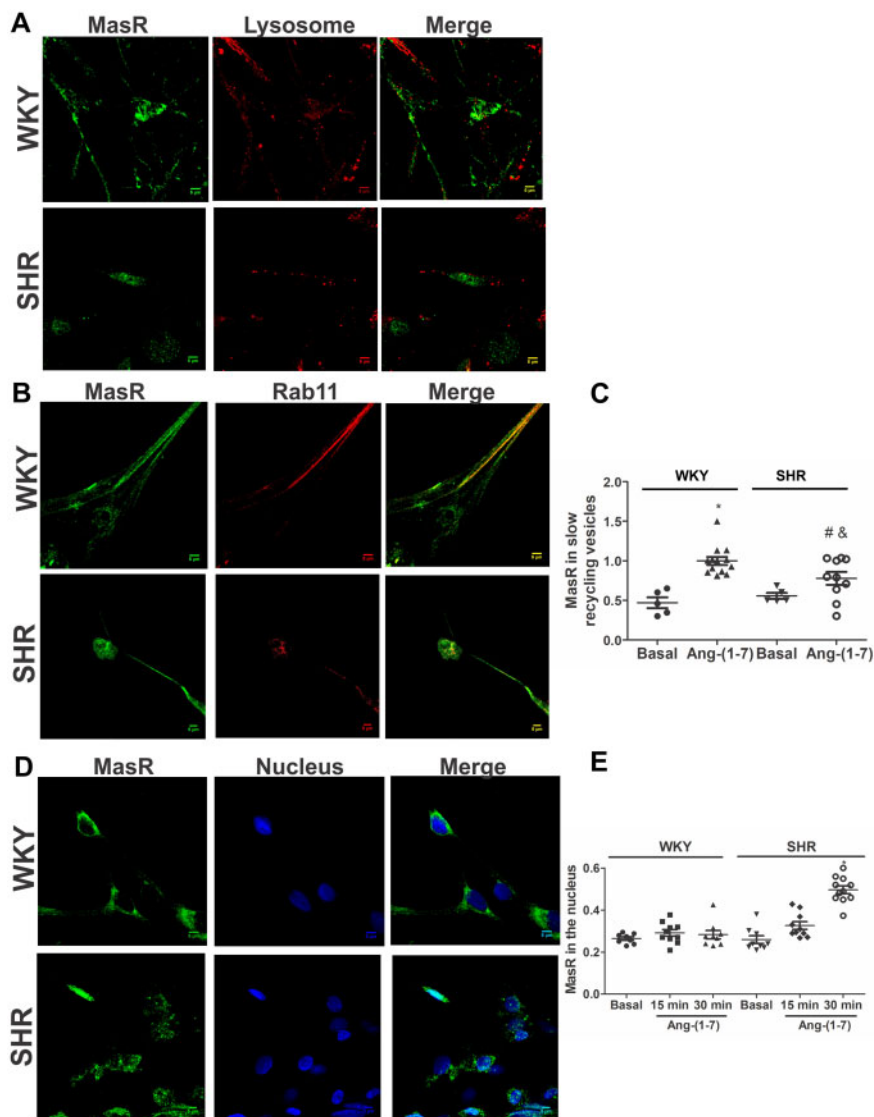


Figure 4 The recycled back fraction of MasR to the plasma membrane is lower in SHR neurons. MasR is translocated to the nucleus in SHR neurons but not in WKY neurons. Representative images of immunostaining of MasR (green) and a lysosome marker (A) or the slow recycling vesicle marker Rab11 (B; red) or the nuclear marker Hoechst (blue; D) in brainstem neurons from WKY rats and SHRs stimulated with Ang-(1-7) for 30 min. Scale bar = 5 μ m. Quantification of MasR colocalization with the slow recycling vesicle marker Rab11 (C) or the nuclear marker Hoechst (E) in brainstem neurons from WKY rats and SHRs incubated in the absence (basal) or the presence of Ang-(1-7) for 30 min (C) or 15 and 30 min (E). The line represents the mean \pm SEM of the ratio between the signals from MasR and Rab 11 (C) or the nuclear marker (E). Four independent experiments were analysed (four to five images per experiment). Experiments were carried out with 500 000 cells for each condition. * $P < 0.05$ vs. WKY; # $P < 0.05$ vs. basal SHR; & $P < 0.05$ vs. Ang-(1-7) WKY (Kruskal–Wallis non-parametric tests followed by Dunn’s multiple comparison tests).

To further confirm MasR translocation to the nucleus, MasR expression was determined by western blot in nuclei isolated from neuronal cells previously incubated in the absence or presence of Ang-(1-7) for 30 min. MasR protein content in the nucleus increased after Ang-(1-7) stimulation in SHR neurons but not in WKY neurons (Figure 6A). To investigate whether MasRs were translocated to the nuclear membrane or inside the nucleus, we evaluated MasR colocalization with Nup62, a nuclear membrane marker, in SHR neurons stimulated for 30 min with Ang-(1-7). MasRs colocalized with Nup62, suggesting that the Rs were present in the nuclear membrane (Figure 6B).

To reinforce the finding that MasRs were translocated to the nucleus after agonist stimulation in neurons from SHRs, nuclear Ang-(1-7) levels in cells previously incubated in the presence of Ang-(1-7) was determined. If MasR translocation to the nucleus occurs, then an increase in nuclear Ang-(1-7) levels may be expected as a result of Ang-(1-7) internalization bound to the R. Under basal conditions, nuclear Ang-(1-7) endogenous levels were greater in SHR neurons than in WKY neurons. After 30 min of Ang-(1-7) stimulation, nuclear Ang-(1-7) levels increased in neurons from SHRs but not in those from WKY rats (Figure 6C). Altogether, these results demonstrate that MasRs are translocated to

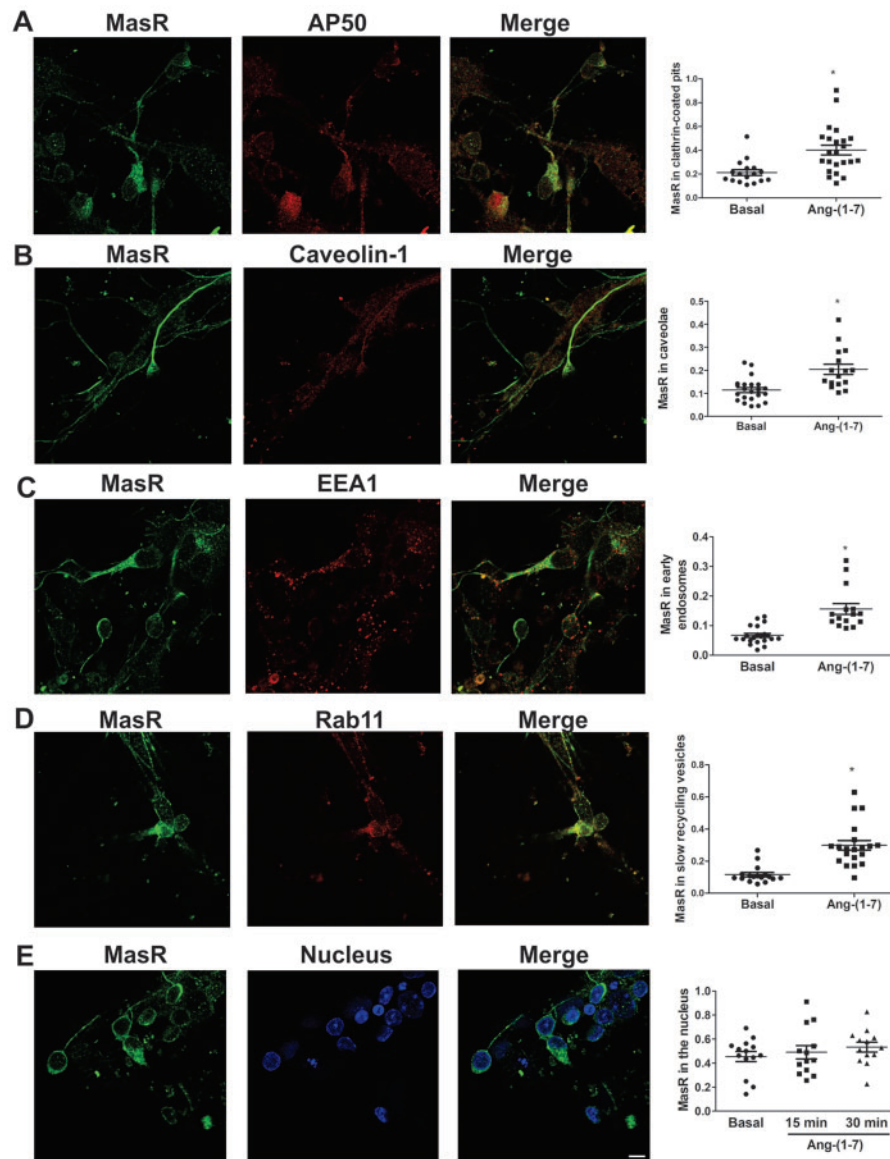


Figure 5 MasR displays the same trafficking in neurons from SD rats as those from WKY rats. Representative images of immunostaining of MasR (green) and the CCP marker AP50 (red; A), the caveolin marker (red; B), the early endosome marker EEA1 (red; C), the slow recycling vesicle marker Rab11 (red; D) or the nuclear marker Hoechst (blue; E) in brainstem neurons from WKY rats and SHRs stimulated with Ang-(1-7) for 15 min (A–C) or 30 min (D and E). Scale bar = 5 μ m. Right graphs represent quantification of MasR colocalization with each marker in brainstem neurons from WKY rats and SHRs incubated in the absence (basal) or the presence of Ang-(1-7) for 15 min (A–C), 30 min (D), or 15 and 30 min (E). The line represents the mean \pm SEM of the ratio between the signals from MasR and the corresponding marker. Four independent experiments were analysed (four to five images per experiment). Experiments were carried out with 500 000 cells for each condition. * $P < 0.05$ vs. basal (Mann–Whitney non-parametric test for A–D; Kruskal–Wallis non-parametric tests followed by Dunn’s multiple comparison tests for E).

the nucleus together with its ligand after agonist stimulation in brainstem neurons from SHRs but not from WKY rats.

4. Discussion

Our study showed that MasRs were internalized into early endosomes in response to agonist stimulation by CCP and caveolae endocytic

pathways and then recycled back to the plasma membrane in brainstem neurons. Importantly, MasRs underwent a different trafficking pattern upon agonist stimulation in SHR neurons: the fraction of MasRs internalized into early endosomes was greater and the fraction of the Rs being recycled back to the plasma membrane was smaller compared with those of the WKY rats. An unpredicted, yet interesting observation is that a fraction of ligand-bound MasRs was translocated to the nucleus only in neurons from SHRs (Figure 7). To our knowledge, this is the first

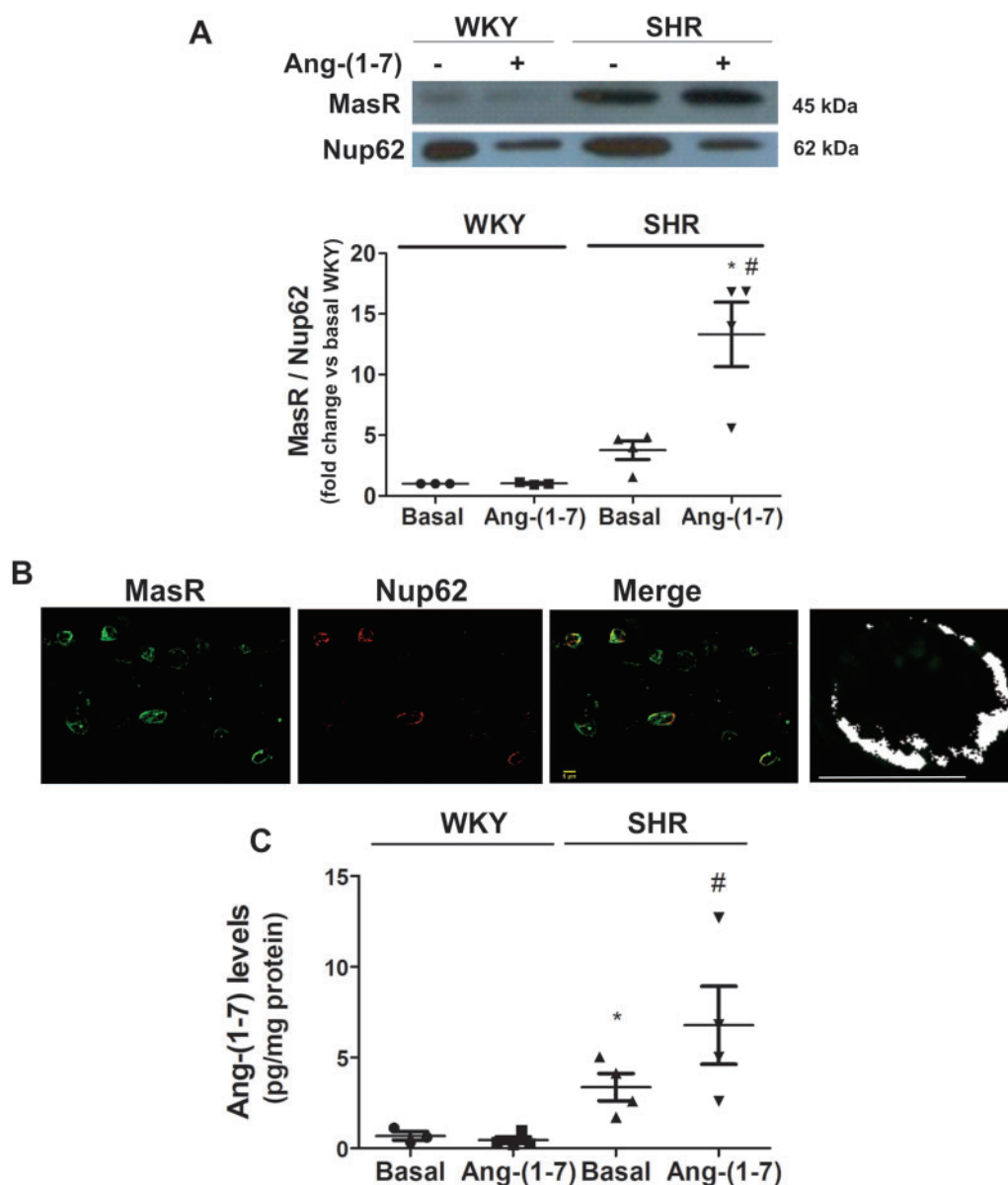


Figure 6 MasR is translocated to the nucleus bound to its agonist. (A) MasR expression in the nuclei from brainstem neurons of WKY rats and SHRs incubated in the absence (basal) or the presence of Ang-(1-7) for 30 min. A representative western blot of MasR and the nuclear pore marker Nup62 is presented. The results are expressed as the fold-change compared with the responses elicited by WKY neurons in the basal condition. The line represents the mean \pm SEM from four independent neuronal cultures (12 million cells per experiment). * $P < 0.05$ compared with the WKY group; # $P < 0.05$ compared with basal SHR (Kruskal–Wallis non-parametric tests followed by Dunn’s multiple comparison tests). (B) Representative images of immunostaining of MasR (green) and Nup62 (nuclear membrane marker) (red) in brainstem neurons of SHRs incubated with 1 $\mu\text{mol/L}$ Ang-(1-7) for 30 min. The last panel corresponds to a representative colocalization map of MasR and Nup62 in the nucleus of one single cell of SHR. The output image produced by the programme contains a map of correlations between pairs of corresponding pixels in two original input images (MasR and Nup62), thereby offering quantitative visualization of colocalization. White dots in the map represent positive correlation (colocalization). This map showed that most of MasRs were present in the nuclear membrane, where every white spot is indicative of a positive colocalization of MasR with the nuclear membrane marker. Scale bar = 5 μm . (C) Nuclear Ang-(1-7) levels from brainstem neurons of WKY rats and SHRs incubated in the absence (basal) or the presence of Ang-(1-7) for 30 min. Results are expressed as pg/mg protein. The line represents the mean \pm SEM from four independent neuronal cultures (12 million cells per experiment). * $P < 0.05$ vs. basal WKY; # $P < 0.05$ vs. basal SHR (Kruskal–Wallis non-parametric tests followed by Dunn’s multiple comparison tests).

report showing agonist-mediated MasR translocation to the nucleus in neurons.

Brainstem neurons from SHRs also showed an increased MasR expression but decreased cellular Ang-(1-7) levels and binding to a putative

Ang-(1-7) receptor (present results). In contrast, AT₁R mRNA expression and Ang II binding were reported to be increased in these neurons.^{31,32} Furthermore, Ang II levels increased in SHR neurons and were significantly higher than those of Ang-(1-7) (present results). Altogether,

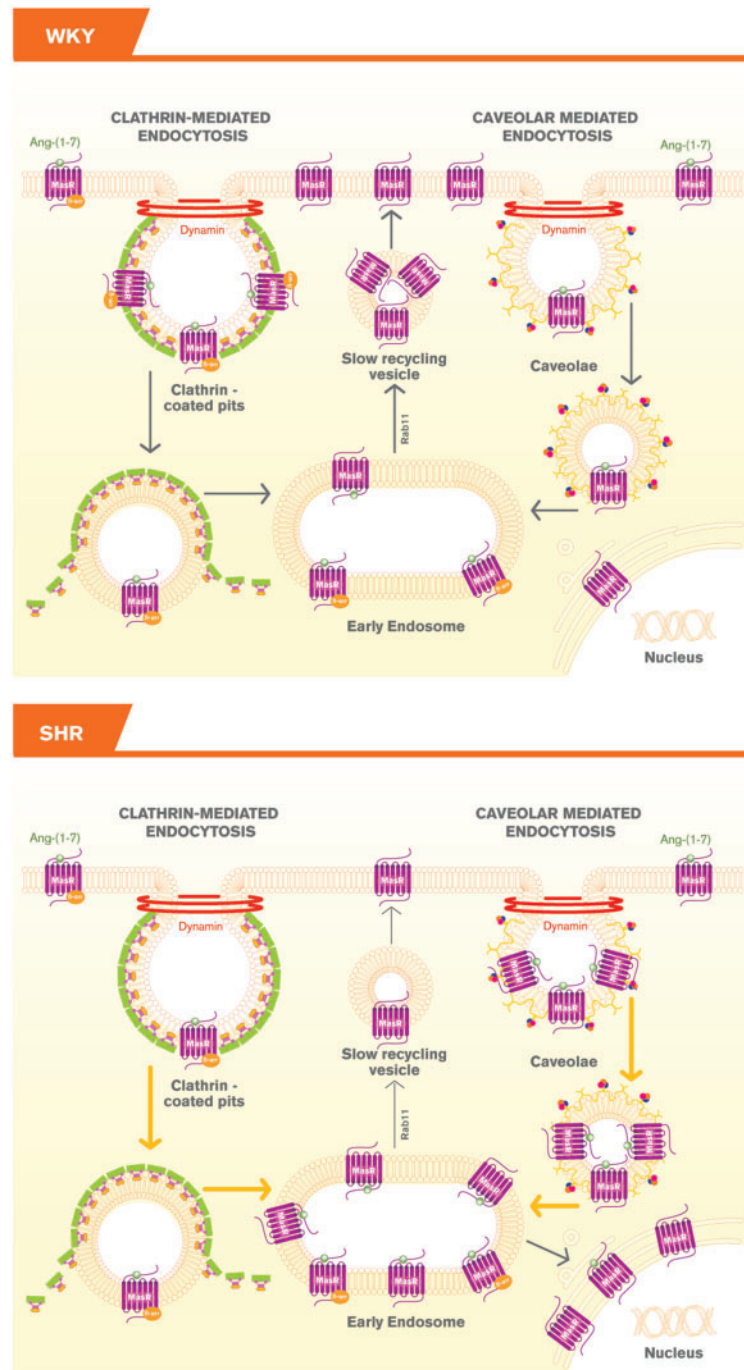
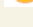




Figure 7 Schematic representation of MasR trafficking in brainstem neurons from WKY and SHR rats. In neurons from WKY rats, MasRs were internalized upon agonist stimulation, targeted to early endosomes and recycled back to the plasma membrane. In neurons from SHRs a greater number of MasRs were internalized, a fraction of MasRs was targeted to the nucleus, whereas a smaller number were recycled back to the plasma membrane.  denotes CCP;  denotes caveolin; and  denotes cavin, which works together with caveolins to regulate caveolae formation.

these data reinforce the concept of an imbalance between the two arms of the RAS in SHRs. The increased MasR expression observed in SHRs neurons may be due to compensate RAS imbalance.

The presence of Ang I, Ang II, renin, angiotensinogen, and Ang II-specific receptors have been shown in cultured neuronal and glial cells from rat brain.^{33–35} An intracellular RAS has also been reported in striatal neurons, astrocytes and microglial cells of rats and monkeys³⁶ and in

dopaminergic neurons in both the monkey and the human substantia nigra.³⁷ Altogether these reports support our finding of endogenous production of Ang-(1-7) in brainstem neurons.

This study was carried out with neuronal cultures obtained from neonates. Although newborn SHRs do not have an established hypertension, this strain has the genetic background to develop hypertension.^{4,38} Ferrari et al.³⁸ found 376 genes differentially expressed between

pre-hypertensive newborn SHR and WKY brainstem neuronal cells that preferentially map to 17 metabolic/signalling pathways. Some of the pathways and regulated genes identified were related to cardiovascular regulation. In fact, ACE mRNA levels are >20-fold higher in cultured neurons from neonatal SHR than in those from WKY,³⁹ the electrophysiological properties of rostral ventrolateral medulla neurons and their responses to Ang II differ between neonatal WKY and SHR neurons⁴⁰ and the neuronal RAS from the brainstem and hypothalamus of SHR differ from WKY rats.³¹ Altogether these results showed that despite the fact that neurons from neonates were used, that is when hypertension is not yet established, the differences observed between both strains were due to the differential genetic background reported for these strains.

In SHR neurons MasR underwent constitutive internalization which was greater when it was mediated through CCP but smaller when it was mediated through caveolae compared with WKY neurons (present results). The increased constitutive R internalization may be due to a greater endogenous Ang-(1-7) tone, but we disregard this hypothesis because Ang-(1-7) levels and its binding to the R were lower in SHR neurons compared with WKY neurons. On the other hand, in SHR neurons the Ang-(1-7)-induced MasR internalization was greater when MasRs were internalized through caveolae but smaller when internalized through CCP. In the end, Ang-(1-7)-mediated MasR internalization in SHR neurons equals to that in WKY neurons. Thus, Ang-(1-7) may compensate the differences in MasR internalization pathways observed in basal conditions in SHR neurons. However, MasR internalization into early endosomes was greater in SHR neurons compared with those from WKY rats, suggesting that another pathway apart from CCP and caveolae may be involved. Together with the fact that the fraction of MasR recycled back to the plasma membrane is lower in SHR neurons, in the end, the amount of MasR inside the cell is greater in SHRs compared with WKY rats.

The Ang-(1-7) reduced binding observed in SHR neurons may explain in part the lack of responses of Ang-(1-7) on NO generation and ERK1/2 and Akt activation in neurons from SHRs. However, the lifetime (or residence time) of the binary drug-target complex, and not the binding affinity *per se*, dictates much of the *in vivo* pharmacological activity.⁴¹ In addition, altered receptor trafficking may contribute as well. Receptor trafficking is pivotal for the temporal and spatial control of GPCR signalling and is regulated by multiple cellular proteins.⁴² Thus, Ang-(1-7)-blunted responses observed in SHRs neurons may result not only from a diminished binding to the R but also from alterations in MasR trafficking. It has been reported that deficiencies in Ang-(1-7) that contribute to autonomic dysfunction were apparent in hypertension and aging.⁴³ The fact that Ang-(1-7) elicits opposite effects on AA release in both strains may be due to different prostaglandins generated in this strain. That is, Ang-(1-7) may induce a decrease in pro-hypertensive prostaglandins as a compensatory mechanism.

Ang-(1-7) was also detected in the nucleus of neurons of both strains, and its levels were higher in SHR neurons compared with those from WKY rats. Nuclear Ang-(1-7) may result in part from the trafficking of the Ang-(1-7)-MasR complex from the plasma membrane to the nucleus (present results) but also from endogenous *de novo* synthesis. Renin, angiotensinogen, ACE2, ACE, Ang II, and Ang-(1-7) were shown to be present in the nucleus of different cellular types.⁴⁴⁻⁴⁷ Nuclear Ang-(1-7) content averaged 57 ± 22 fmol/mg in NRK-52E renal epithelial cells,⁴⁷ which was near 25-fold higher than those observed in brainstem neurons, and this may be due to differences in the cell type.

Our study showed that MasRs were expressed in the nuclei of neurons. MasR expression has been described to be present in the nuclei of

renal cortical cells in sheep,⁴⁴ in NRK-52E renal epithelial cells,⁴⁷ and in different neuronal and glial cell types.⁴⁶ Neither of these reports has shown MasR translocation to the nucleus upon agonist stimulation. Nuclear GPCRs participate in nuclear signalling and can alter gene expression.^{29,30} It has been reported that nuclear Ang-(1-7) stimulates NO and this response is reduced in aged animals or those with foetal programmed hypertension.^{43,44} In rat nigral isolated nuclei MasR activation by Ang-(1-7) induced an increase in nuclear NO production, counteracted the increase in Ang II-derived nuclear superoxide generation and decreased the expression of mRNA for AT₂Rs.⁴⁶ Since Ang-(1-7) induces NET gene expression through MasR stimulation in hypothalamic and brainstem neurons of SHRs,⁴⁸ we cannot disregard that this effect may result from MasR translocation to the nucleus. The implications of MasR nuclear trafficking in SHR neurons remains to be clarified. Our ongoing experiments are focused to elucidate nuclear MasR-mediated responses.

Many theories have been proposed to explain GPCR translocation to the nucleus,^{29,30} but still, little is known about the exact mechanisms. MasRs are thought to be localized, at least in part, to the outer nuclear membrane in sheep renal cortex nuclei because of their rapid response to Ang-(1-7) stimulation in isolated nuclei.⁴⁴ This study showed that after agonist stimulation, nuclear MasRs were mostly colocalized with Nup62, a nuclear pore complex protein. This suggests that the Rs are using this pathway to enter the nucleus, as it was previously shown for AT₁Rs.⁴⁹

In conclusion, our report showed that upon Ang-(1-7) stimulation, MasRs were internalized, targeted to early endosomes and recycled back to the plasma membrane in brainstem neurons from WKY rats and SHRs. However, MasRs displayed a differential trafficking in neurons from SHRs rats: a greater number of MasRs were internalized into early endosomes while a smaller number were recycled back to the plasma membrane, which may result in a smaller number of re-sensitized Rs present in the plasma membrane. This may explain in part the blunted or absent responses of Ang-(1-7) in SHR neurons. Furthermore, a fraction of MasRs was targeted to the nucleus only in neurons from SHRs and in this case, cells internalized the R together with its ligand (Figure 7). The differential trafficking of MasRs in SHR neurons may be a compensatory mechanism to overcome hypertension.

Supplementary material

Supplementary material is available at *Cardiovascular Research* online.

Conflict of interest: none declared.

Funding

This work was supported by grants from Universidad de Buenos Aires [20020160100134BA to M.M.G.]; Agencia Nacional de Promoción Científica y Tecnológica [2013-2170 and 2016-2978 to M.M.G.]; and National Institutes of Health [HL028982 to O.A.C.].

References

- Nakagawa P, Sigmund CD. How is the brain renin-angiotensin system regulated? *Hypertension* 2017;**70**:10–18.
- Santos RAS, Sampaio WO, Alzamora AC, Motta-Santos D, Alenina N, Bader M, Campagnole-Santos MJ. The ACE2/angiotensin-(1-7)/MAS axis of the renin-angiotensin system: focus on angiotensin-(1-7). *Physiol Rev* 2018;**98**:505–553.
- Gironacci MM, Longo Carbajosa NA, Goldstein J, Cerrato BD. Neuromodulatory role of angiotensin-(1-7) in the central nervous system. *Clin Sci* 2013;**125**:57–65.

4. Okuda T, Sumiya T, Iwai N, Miyata T. Difference of gene expression profiles in spontaneous hypertensive rats and Wistar-Kyoto rats from two sources. *Biochem Biophys Res Commun* 2002;**296**:537–543.
5. Amenta F, Di Tullio MA, Tomassoni D. Arterial hypertension and brain damage—evidence from animal models (review). *Clin Exp Hypertens* 2003;**25**:359–380.
6. West C, Hanyaloglu AC. Minireview: spatial programming of G protein-coupled receptor activity: decoding signaling in health and disease. *Mol Endocrinol* 2015;**29**:1095–1106.
7. Scita G, Di Fiore PP. The endocytic matrix. *Nature* 2010;**463**:464–473.
8. Cerniello FM, Carretero OA, Longo Carbajosa NA, Cerrato BD, Santos RA, Grecco HE, Gironacci MM. MAS1 receptor trafficking involves ERK1/2 activation through a beta-arrestin2-dependent pathway. *Hypertension* 2017;**70**:982–989.
9. Gironacci MM, Adamo HP, Corradi G, Santos RA, Ortiz P, Carretero OA. Angiotensin (1-7) induces MAS receptor internalization. *Hypertension* 2011;**58**:176–181.
10. Bunnett NW, Cottrell GS. Trafficking and signaling of G protein-coupled receptors in the nervous system: implications for disease and therapy. *CNS Neurol Dis Drug Targets* 2010;**9**:539–556.
11. Tang BL. Rabs, membrane dynamics, and Parkinson's disease. *J Cell Physiol* 2017;**232**:1626–1633.
12. Burghi V, Fernández NC, Gándola YB, Piazza VG, Quiroga DT, Guilhen Mario É, Felix Braga J, Bader M, Santos RAS, Dominici FP, Muñoz MC. Validation of commercial Mas receptor antibodies for utilization in Western Blotting, immunofluorescence and immunohistochemistry studies. *PLoS One* 2017;**12**:e0183278.
13. Doggrel SA, Brown L. Rat models of hypertension, cardiac hypertrophy and failure. *Cardiovasc Res* 1998;**39**:89–105.
14. Aiello EA, Villa-Abrille MC, Escudero EM, Portiansky EL, Perez NG, de Hurtado MC, Cingolani HE. Myocardial hypertrophy of normotensive Wistar-Kyoto rats. *Am J Physiol Heart Circ Physiol* 2004;**286**:H1229–H1235.
15. Qualy JM, Westfall TC. Release of norepinephrine from the paraventricular hypothalamic nucleus of hypertensive rats. *Am J Physiol* 1988;**254**:H993–H1003.
16. Lopez Verrilli MA, Pirola CJ, Pascual MM, Dominici FP, Turyn D, Gironacci MM. Angiotensin-(1-7) through AT receptors mediates tyrosine hydroxylase degradation via the ubiquitin-proteasome pathway. *J Neurochem* 2009;**109**:326–335.
17. Guadagnoli T, Caltana L, Vacotto M, Gironacci MM, Brusco A. Direct effects of ethanol on neuronal differentiation: an *in vitro* analysis of viability and morphology. *Brain Res Bull* 2016;**127**:177–186.
18. Ichikawa M, Muramoto K, Kobayashi K, Kawahara M, Kuroda Y. Formation and maturation of synapses in primary cultures of rat cerebral cortical cells: an electron microscopic study. *Neurosci Res* 1993;**16**:95–103.
19. Moutaux E, Christaller W, Scaramuzzino C, Genoux A, Charlot B, Cazorla M, Saudou F. Neuronal network maturation differently affects secretory vesicles and mitochondria transport in axons. *Sci Rep* 2018;**8**:13429.
20. Brosnihan KB, Chappell MC. Measurement of angiotensin peptides: HPLC-RIA. *Methods Mol Biol* 2017;**1527**:81–99.
21. Gironacci MM, Brosnihan KB, Ferrario CM, Gorzalczy S, Verrilli MA, Pascual M, Taira C, Pena C. Increased hypothalamic angiotensin-(1-7) levels in rats with aortic coarctation-induced hypertension. *Peptides* 2007;**28**:1580–1585.
22. Gironacci MM, Coba MP, Pena C. Angiotensin-(1-7) binds at the type 1 angiotensin II receptors in rat renal cortex. *Regul Peptides* 1999;**84**:51–54.
23. Santos RA, Simoes e Silva AC, Maric C, Silva DM, Machado RP, de Buhr I, Heringer-Walther S, Pinheiro SV, Lopes MT, Bader M, Mendes EP, Lemos VS, Campagnole-Santos MJ, Schultheiss HP, Speth R, Walther T. Angiotensin-(1-7) is an endogenous ligand for the G protein-coupled receptor Mas. *Proc Natl Acad Sci USA* 2003;**100**:8258–8263.
24. Cerrato BD, Carretero OA, Janic B, Grecco HE, Gironacci MM. Heteromerization between the Bradykinin B2 receptor and the angiotensin-(1-7) Mas receptor: functional consequences. *Hypertension* 2016;**68**:1039–1048.
25. Shulei W, Arena ET, Eliceiri KW, Ming Y. Automated and robust quantification of colocalization in dual-color fluorescence microscopy: a nonparametric statistical approach. *IEEE Trans Image Process* 2018;**27**:622–636.
26. Dunn KW, Kamocka MM, McDonald JH. A practical guide to evaluating colocalization in biological microscopy. *Am J Physiol Cell Physiol* 2011;**300**:C723–C742.
27. Zinchuk V, Zinchuk O, Okada T. Quantitative colocalization analysis of multicolor confocal immunofluorescence microscopy images: pushing pixels to explore biological phenomena. *Acta Histochem Cytochem* 2007;**40**:101–111.
28. Nothwang HGG, Schindler J. Subcellular fractionation of small sample amounts. In JM Walker (ed.), *The Protein Protocols Handbook*. Totowa: Springer, Humana Press; 2009. pp. 165–170.
29. Campden R, Audet N, Hebert TE. Nuclear G protein signaling: new tricks for old dogs. *J Cardiovasc Pharmacol* 2015;**65**:110–122.
30. Jong YI, Harmon SK, O'Malley KL. GPCR signalling from within the cell. *Br J Pharmacol* 2018;**175**:4026–4035.
31. Ferrari MF, Raizada MK, Fior-Chadi DR. Nicotine modulates the renin-angiotensin system of cultured neurons and glial cells from cardiovascular brain areas of Wistar Kyoto and spontaneously hypertensive rats. *J Mol Neurosci* 2007;**33**:284–293.
32. Raizada MK, Lu D, Tang W, Kurian P, Summers C. Increased angiotensin II type-1 receptor gene expression in neuronal cultures from spontaneously hypertensive rats. *Endocrinology* 1993;**132**:1715–1722.
33. Hermann K, Raizada MK, Summers C, Phillips MI. Immunocytochemical and biochemical characterization of angiotensin I and II in cultured neuronal and glial cells from rat brain. *Neuroendocrinology* 1988;**47**:125–132.
34. Hermann K, Raizada MK, Summers C, Phillips MI. Presence of renin in primary neuronal and glial cells from rat brain. *Brain Res* 1987;**437**:205–213.
35. Kumar A, Rassoli A, Raizada MK. Angiotensinogen gene expression in neuronal and glial cells in primary cultures of rat brain. *J Neurosci Res* 1988;**19**:287–290.
36. Garrido-Gil P, Rodriguez-Perez AI, Fernandez-Rodriguez P, Lanciego JL, Labandeira-Garcia JL. Expression of angiotensinogen and receptors for angiotensin and prorenin in the rat and monkey striatal neurons and glial cells. *Brain Struct Funct* 2017;**222**:2559–2571.
37. Garrido-Gil P, Valenzuela R, Villar-Cheda B, Lanciego JL, Labandeira-Garcia JL. Expression of angiotensinogen and receptors for angiotensin and prorenin in the monkey and human substantia nigra: an intracellular renin-angiotensin system in the nigra. *Brain Struct Funct* 2013;**218**:373–388.
38. Ferrari MF, Reis EM, Matsumoto JP, Fior-Chadi DR. Gene expression profiling of cultured cells from brainstem of newborn spontaneously hypertensive and Wistar Kyoto rats. *Cell Mol Neurobiol* 2009;**29**:287–308.
39. King SJ, Oparil S, Berecek KH. Neuronal angiotensin-converting enzyme (ACE) gene expression is increased by converting enzyme inhibitors (CEI). *Mol Cell Neurosci* 1991;**2**:13–20.
40. Matsuura T, Kumagai H, Kawai A, Onimaru H, Imai M, Oshima N, Sakata K, Saruta T. Rostral ventrolateral medulla neurons of neonatal Wistar-Kyoto and spontaneously hypertensive rats. *Hypertension* 2002;**40**:560–565.
41. Copeland RA. The drug-target residence time model: a 10-year retrospective. *Nat Rev Drug Discov* 2016;**15**:87–95.
42. Sposini S, Hanyaloglu AC. Evolving view of membrane trafficking and signaling systems for G protein-coupled receptors. *Prog Mol Subcell Biol* 2018;**57**:273–299.
43. Chappell MC, Marshall AC, Alzayadneh EM, Shaltout HA, Diz DI. Update on the angiotensin converting enzyme 2-Angiotensin (1-7)-MAS receptor axis: fetal programming, sex differences, and intracellular pathways. *Front Endocrinol* 2014;**4**:201.
44. Gwathmey TM, Alzayadneh EM, Pendergrass KD, Chappell MC. Novel roles of nuclear angiotensin receptors and signaling mechanisms. *Am J Physiol Regul Integr Comp Physiol* 2012;**302**:R518–R530.
45. Camargo de Andrade MC, Di Marco GS, de Paulo Castro Teixeira V, Mortara RA, Sabatini RA, Pesquero JB, Boim MA, Carmona AK, Schor N, Casarini DE. Expression and localization of N-domain ANG I-converting enzymes in mesangial cells in culture from spontaneously hypertensive rats. *Am J Physiol Renal Physiol* 2006;**290**:F364–F375.
46. Costa-Besada MA, Valenzuela R, Garrido-Gil P, Villar-Cheda B, Parga JA, Lanciego JL, Labandeira-Garcia JL. Paracrine and intracrine angiotensin 1-7/Mas receptor axis in the substantia nigra of rodents, monkeys, and humans. *Mol Neurobiol* 2018;**55**:5847–5867.
47. Alzayadneh EM, Chappell MC. Nuclear expression of renin-angiotensin system components in NRK-52E renal epithelial cells. *J Renin Angiotensin Aldosterone Syst* 2015;**16**:1135–1148.
48. Lopez Verrilli MA, Rodriguez Fermepin M, Longo Carbajosa N, Landa S, Cerrato BD, García S, Fernandez BE, Gironacci MM. Angiotensin-(1-7) through Mas receptor up-regulates neuronal norepinephrine transporter via Akt and Erk1/2-dependent pathways. *J Neurochem* 2012;**120**:46–55.
49. Lu D, Yang H, Shaw G, Raizada MK. Angiotensin II-induced nuclear targeting of the angiotensin type 1 (AT1) receptor in brain neurons. *Endocrinology* 1998;**139**:365–375.

Translational perspective

R trafficking is not a universal mechanism for every R and it critically determines the ultimate cellular response. Alterations in R trafficking have been associated with several diseases, hypertension and neurodegenerative diseases among others. We provide evidence, for the first time, about MasR trafficking in brainstem neurons from SHR. This work opens the way in comprehending the mechanisms underlying MasR regulation in a pathological situation. The differential MasR trafficking in neurons from SHR may contribute to the impaired responses of Ang-(1-7) and to hypertension development.